Temperature cycling effects between Sn/Pb solder and electroless copper plated AlN substrate

Bi-SHIOU CHIOU
Department of Electronics Engineering and Institute of Electronics, National Chiao Tung University, Hsinchu, Taiwan

JIANN-HAUR CHANG and JENQ-GONG DUH
Department of Materials Science and Engineering, National Tsing Hua University, Hsinchu,Taiwan

Thermal cycling effects on Sn/Pb solder and electroless Cu-plated AlN substrates are investigated. X-ray diffraction patterns reveal the existence of Cu_2O for the electroless Cu-plated AlN after thermal cycling in an environmental chamber. Moisture in the chamber results in the oxidation of electroless plated Cu and fracture takes place at the Cu_2O/Cu interface. The oxidation of Cu is also confirmed by Auger depth profile and electrical sheet resistance measurement. For the solder/Cu/AlN system, fracture occurs at the Cu/solder interface. No intermetallic compounds between solder and Cu are found after thermal cycling. Stress resulting from the thermal expansion mismatch is the major cause of loss of adhesion

1. Introduction

The need for smaller and more reliable integrated circuits and higher voltage devices for power applications have been the trend of the electronics industry in recent years. Aluminium nitride, with its high thermal conductivity, adequate mechanical strength, good insulation resistance and a thermal expansion coefficient close to that of silicon, has attracted much attention for use as a substrate material [1–4]. Electroless Cu plating provides an excellent approach to metallizing the ceramic substrate. Previous works by Chiou, Chang and Duh reported that the adhesion strength of the electroless plated Cu to AlN substrate is much larger than 19.6 N mm^{-2}, which is generally needed for the mounting of circuit devices [5, 6].

Interconnections between the conductor metallization and discrete electronic devices are frequently made through a solder alloy screen-printed or soldered into position. During the soldering operation and subsequent joint life, intermetallic compounds form and grow. The metallurgical reactions between the solder and conductor metallization might have a deleterious effect on the adhesion of the conductor to the underlying substrate, particularly when the assemblies are subjected to thermal ageing and temperature cycling [7-14]

This work is part of a continuing investigation undertaken to establish and to minimize potential reliability problems arising from the use of soldered electroless Cu-plated AlN in electronic packages. The first phase of this work, reported in previous papers [5, 6, 14], described the adhesion mechanism at the electroless plated Cu/AlN interface and the effect of intermetallic formation on the Sn/Pb solder and Cu conductor interfaces after thermal storage. The present paper deals with temperature cycling effects on the Sn/Pb solder and Cu conductor metallizations.

2. Experimental procedure

The Cu conductor was electroless plated on the aluminium nitride substrate. Details for the pretreatment of the AlN substrate before plating, the plating procedures and the plating conditions have been described elsewhere [6, 14]. Copper films of ~ 10 µm thickness were deposited on etched AlN substrates which exhibited a surface roughness of ~ 0.13 µm

The electroless copper-plated specimens were cleaned in deionized water in an ultrasonic cleaner for 10 min., and then dipped into the RMA (4381 RAM-type, multicore, Herfordshire, England) flux. The solder was a 63Sn/37Pb eutectic alloy (SN63 eutectic, Multicore, Hertfordshire, England), and the solder bath was held at 230 °C. The substrate was vertically dipped into the bath for five seconds. The soldered specimens were then cleaned with a cleaning agent (PC81 cleaner, Multicore, Hertfordshire, England) in an ultrasonic cleaner for 20 min. The as-plated and/or soldered samples were then subjected to the thermal cycle test. The adhesion strength of the Cu deposited on to the AlN substrate was evaluated after various cycles by the pull-off test [6, 14]. Two types of thermal cycle test were performed in this study. One was carried out in an environmental chamber with a four-hour cyclic period from − 50 °C to 150 °C and was designated as slow thermal cycling. The other was
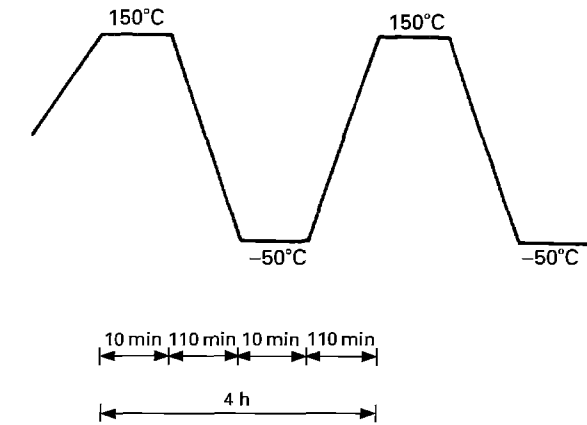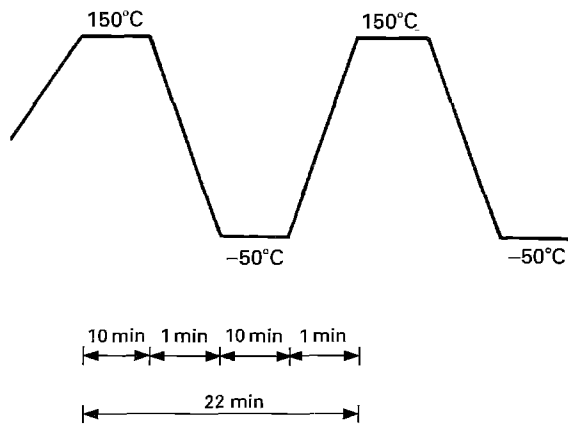
Figure 1 Temperature profiles for (a) slow thermal cycling and (b) fast thermal cycling.

Figure 2 Adhesion strength of electroless plated Cu to AlN substrate after the slow thermal cycling test.

performed with a 22 min cyclic period (designed as fast thermal cycling) from $-50\,°C$ to $150\,°C$ between the freezing chamber and the oven. Temperature profiles for these two cycling tests are shown in Fig. 1. Thickness measurements were done with an α-step surface profile measuring system (Alpha-step 250, Tencor, U.S.A). The sheet resistance of the Cu film was evaluated with a conventional four-point probe (Model RT-7, Napson, Japan), which was a linear array of equally spaced probes (probe spacing $S = 1$ mm).

The phase and crystal structure of the sample assembly were identified with an X-ray diffractometer (D/MAX-B, Rigaku, Japan) with CuKα radiation at 0.154 nm. The surface morphology and cross-sectional view morphology were observed with a scanning electron moicroscope (SEM, Camscan, England) equipped with an EDX analyser (Excel, Link, England). In addition the compositional depth profile was recorded by Auger electron spectroscopy (PHI-590AM Scanning Auger Microprobe, Perkin-Elmer, U.S.A). The depth profiles of Cu and O were used to determine the thickness of the oxidized layer on the electroless copper.
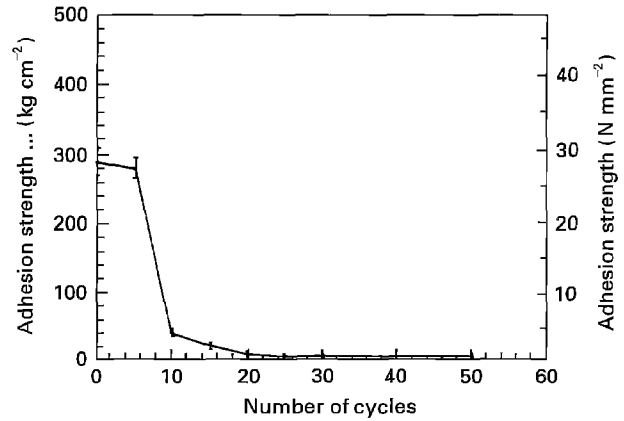
3. Results and discussion

The difference in the thermal expansion coefficients is always attributed as the reason for joint failure under thermal cycling. Stress resulting from thermal mismatch tends to reduce the adhesion between the deposit and the substrate. The thermal expansion coefficients of AlN, Cu and 63Sn/37Pb are $4.6 \times 10^{-6}\,°C^{-1}$, $24.7 \times 10^{-6}\,°C^{-1}$, and $16.6 \times 10^{-6}\,°C^{-1}$, respectively [1, 15, 16]. To investigate the reliability of the electroless Cu-plated AlN, specimens were placed in an environmental chamber for the thermal cycling test. The adhesion strength of electroless plated Cu to AlN after temperature cycling is given in Fig. 2. The adhesion strength drops below 4.9 Nmm^{-2} after 10 cycles.

The X-ray diffraction patterns of electroless Cu-plated AlN after various cycles are shown in Fig. 3. The Cu_2O phase is found after 10 cycles and the amount of Cu_2O is enhanced as the number of cycles is increased. Fig. 4 demonstrates Auger depth profiles of Cu and O for specimens subjected to 5, 10 and 15 thermal cycles. The oxidized layer reaches ∼ 650 nm when the number of cycles is 15. It is observed that fracture takes place at the Cu side, instead of at the Cu/AlN interface after the pull-off test, for samples subjected to more after 10 cycles. The X-ray diffraction patterns from the fracture surface for samples after 20 cycles are represented in Fig. 5. There exists primarily Cu_2O with negligible Cu on the top fracture surface. The top fracture surface is the one attached to the stud after fracture, while the bottom fracture surface is associated with the underlying substrate. The Al phase indicated in Fig. 5 comes from the stud used for the pull-off test. On the bottom fracture surface, however, Cu and AlN phases are identified, while Cu_2O is not observed. This implies that the crack propagates through the Cu_2O/Cu interface. It is argued that forming Cu_2O on the electroless Cu surface alters the mechanical properties of electroless Cu, and thus the electroless Cu becomes brittle. As a consequence, fracture takes place within the deposit itself.

In addition, the presence of Cu_2O on electroless Cu increases the electrical resistance of the electroless Cu. The sheet resistance of the deposits after various numbers of cycles is shown in Fig. 6. The sheet resistance
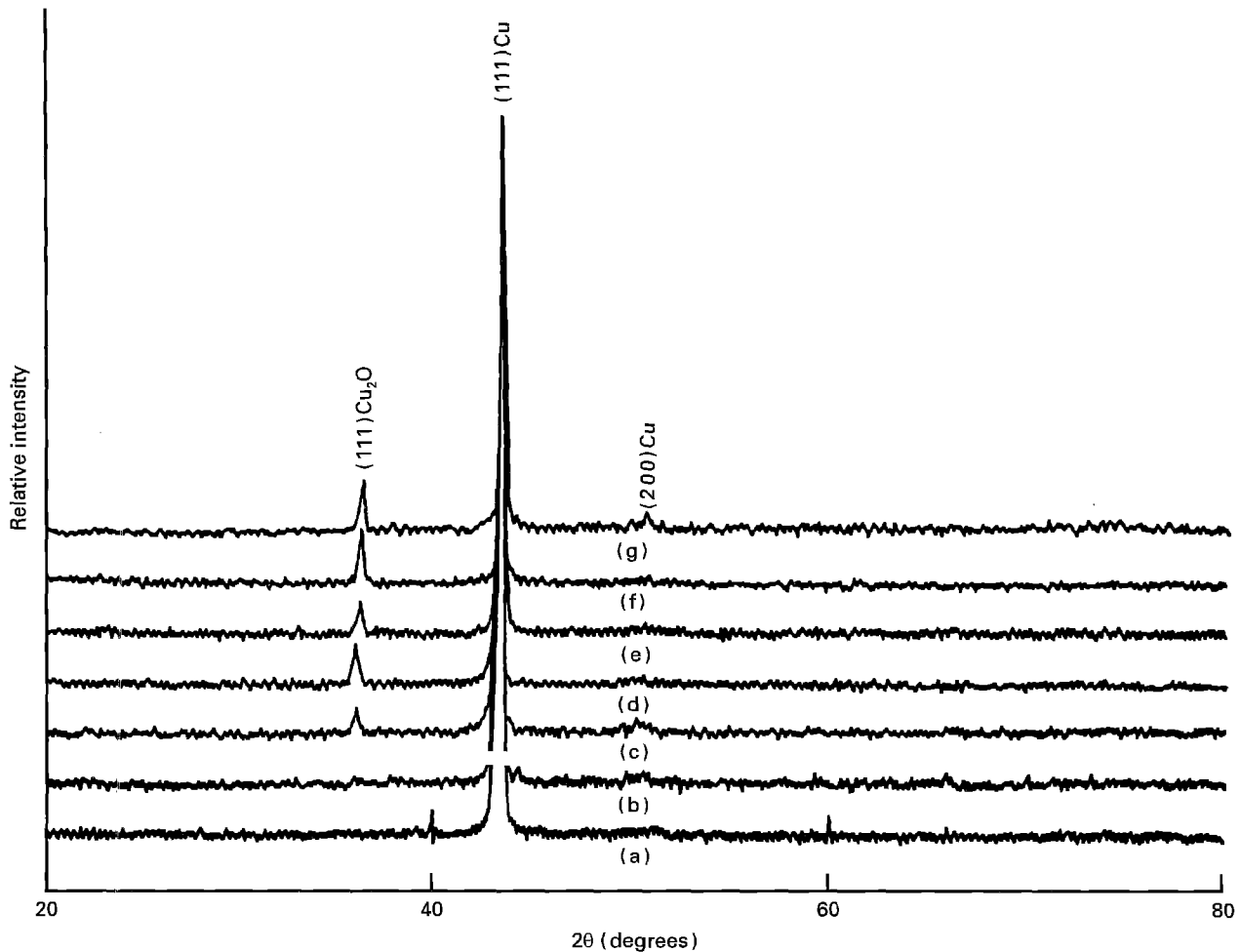
Figure 3 X-ray diffraction patterns of the electroless Cu-plated AlN substrate after various slow thermal cycles in an environmental chamber. (a) 0 cycles, (b) 5 cycles, (c) 10 cycles, (d) 15 cycles, (e) 20 cycles, (f) 25 cycles, and (g) 30 cycles.
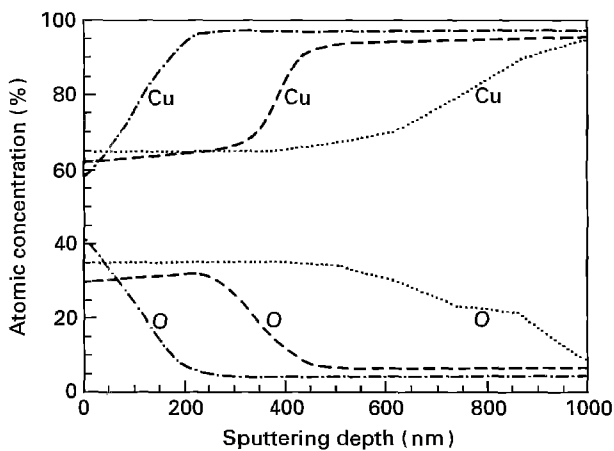

Figure 4 Auger depth profiles of Cu and O for the electroless Cu plated AlN substrate after (−·−) (5), (−−−) (10), and (···) (15), slow thermal cycles.

of the deposit increases drastically after 10 thermal cycles due to the formation of Cu_2O.

The slow thermal cycling test was performed in an environmental chamber. The moisture existing in the environmental chamber freezes to ice when the temperature is dropped from the elevated temperature (150 °C) to the lower temperature (− 50 °C). On the

other hand, when the temperature is increased from − 50 °C to 150 °C, the ice melts and water vaporizes. It is argued that the oxidation of copper is attributed to the presence of moisture. In order to investigate this possibility, another temperature profile, shown in Fig. 1b, was employed. Specimens were transferred manually from an oven at 150 °C to freezing chamber at − 50 °C with a cyclic period of 22 min. The Cu_2O phase is not observed in X-ray diffraction patterns for these samples under fast thermal cycling conditions. Fig. 7 indicates the variation in the measurement of the adhesion strength after fast thermal cycling. The sample fails at the Cu/AlN interface after the pull-off test. The adhesion strength decreases gradually as the number of thermal cycles increases, and it decreases to below 4.9 Nmm^{-2} after 25 cycles.

As a comparison, the adhesion strength after 5 cycles is 27.4 Nmm^{-2} for slow thermal cycling, while it is only 15.2 Nmm^{-2} for the fast thermal cycling. The duration of the temperature transient between 150 °C and − 50 ° C is 110 min for the slow thermal cycles as compared to only 1 min for the fast cycling; thus more thermal shock is introduced in the fast cycling than in the slow cycling. This is the reason why the adhesion strength after 5 cycles of fast cycling is lower than that for slow cycling. As the number of thermal cycles increases to 10, the adhesion strength for slow cycling
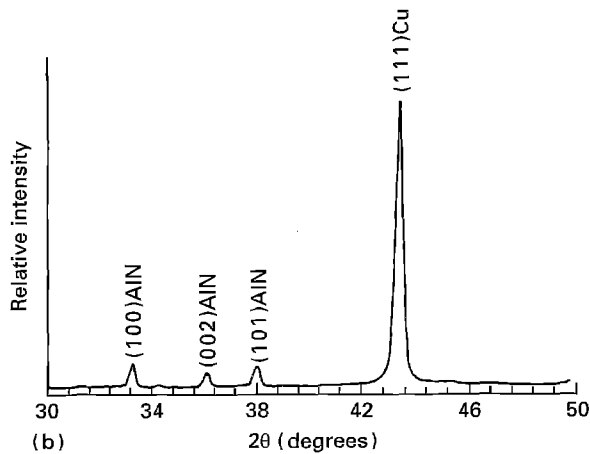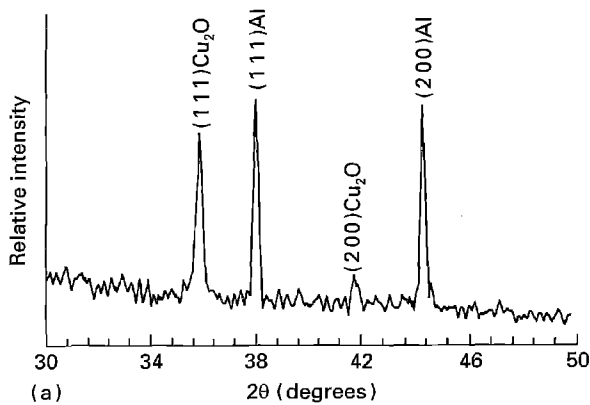
377

Figure 5 X-ray diffraction patterns of the fracture surface for the electroless Cu-plated AlN substrate after 20 slow thermal cycles. (a) Top fracture srface and (b) bottom fracture surface.
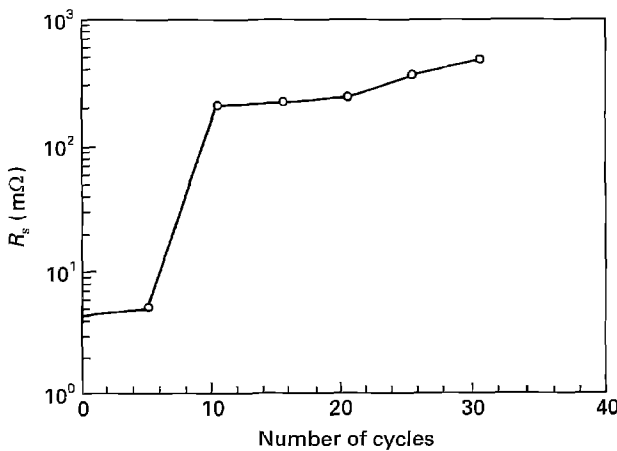

Figure 6 Sheet resistance of the electroless plated Cu after various numbers of slow thermal cycles.
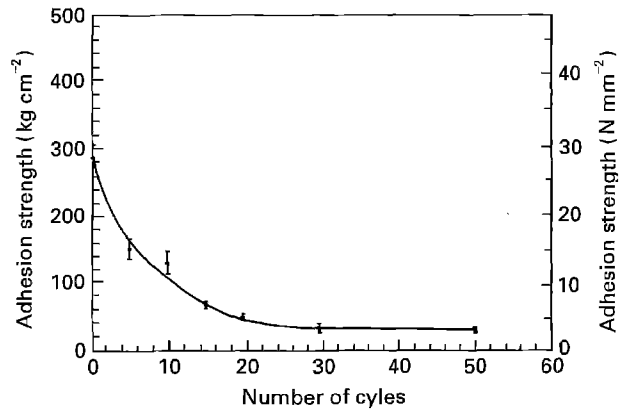

Figure 7 The adhesion strength of electroless Cu-plated AlN substrate after various numbers of fast thermal cycles.
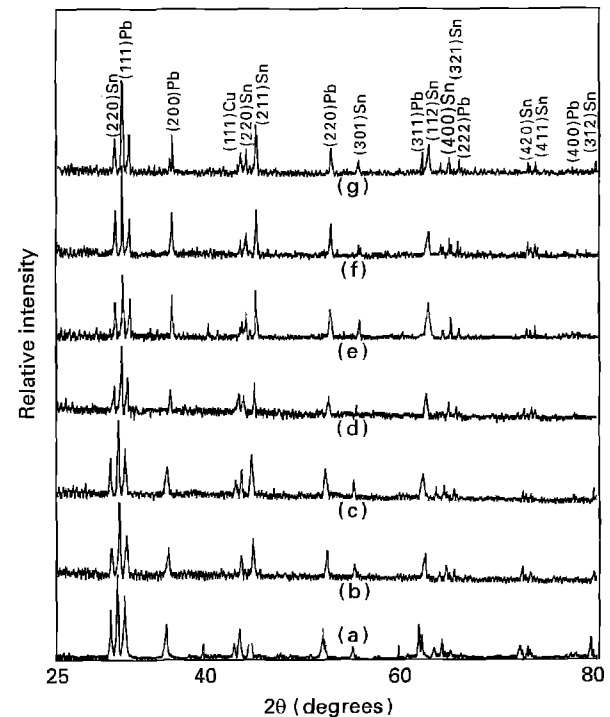

Figure 8 X-ray diffraction patterns of soldered samples after various numbers of slow thermal cycles. (a) 0 cycles, (b) 5 cycles, (c) 10 cycles, (d) 15 cycles, (e) 20 cycles, (f) 25 cycles and (g) 30 cycles.

decreases to 3.9 Nmm^{-2} while it is 12.9 Nmm^{-2} for fast cycling. One might argue that the dramatic decrease in the adhesion strength after slow cycling results from the oxidation of electroless Cu. On the other hand, the sample subjected to fast cycling is not affected significantly by moisture. Thus the adhesion strength is higher than that for slow cycling after more than 10 cycles.

Fig. 8 demonstrates the X-ray diffraction patterns of soldered specimens after various numbers of slow thermal cycles. No intermetallic compound is found

in the solder/Cu/AlN system after 30 cycles. Cu_2O phase is not observed since the electroless Cu surface is covered by solder. The adhesion strength, shown in Fig. 9, decreases to below 4.9 Nmm^{-2} after 25 cycles. The cross-sectional view of the fracture surface after the pull-off test is represented in Fig. 10. The fracture takes place at the Cu/solder, interface. Since no intermetalic is formed between the Cu layer and the solder, as is the case for soldered sample after thermal storage [14], the main cause for failure should be the thermal stress resulting from thermal cycling. It is believed that the difference in thermal expansion between the Cu plating and the solder introduces appreciable thermal stresses when the sample is subjected to the thermal cycling test, and the resulting thermal stress in the deposit causes the adhesion strength to degrade, as indicated in Fig. 9.
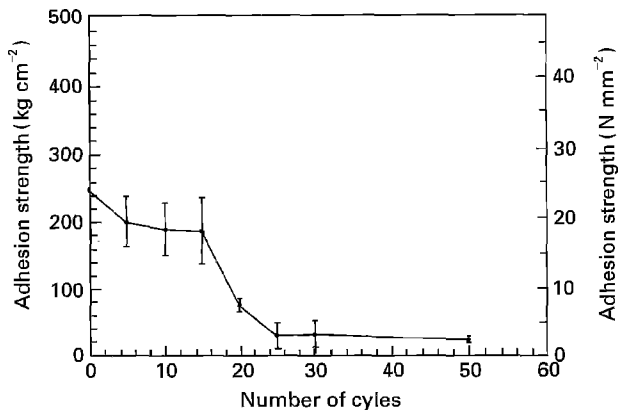
Figure 9 Adhesion strength of soldered samples after various numbers of slow thermal cycles.
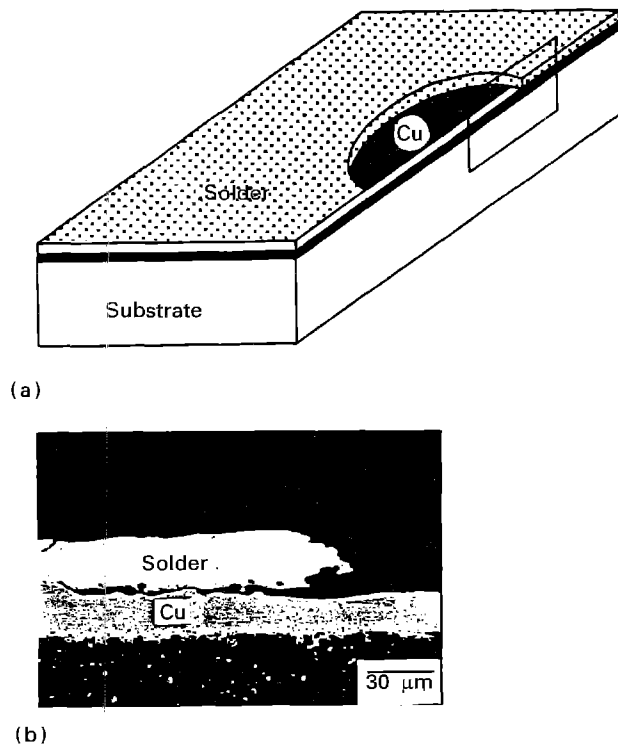

(a)

(b)

Figure 10 The cross-sectional view of the fracture surface of the soldered samples after the pull-off test. Samples subjected to 30 slow thermal cycles. (a) Schematic diagram and (b) SEM morphology

4. Conclusion

Temperature cycling effects between the Sn/Pb solder and the electroless Cu-plated AlN substrate are evaluated. During the thermal cycling test, oxidation of electroless Cu takes place due to moisture in the environmental chamber. Cu_2O is thus formed on the

electroless Cu and results in a decrease in the adhesion strength and an increase in the electrical sheet resistance. During the pull-off test, the crack propagates through the Cu_2O/Cu interface and fracture takes place within the plated Cu. For soldered specimens after 30 thermal cycles, no intermetallic compound is found and the loss in adhesion strength is attributed to the thermal stress as caused by the temperature transient.

Acknowledgement

References

1. L. M. SHEPPARD, Ceram. Bull. 69, (11) (1990) 1881.
2. R. R. TUMMALA, in "Ceramic substrates and packages for electronic applications", Adv. in Ceramics, Vol.26, edited by M. F. YAN, K. NIWA, H. M. O'BRYAN Jr and W. S. YOUNG. (The American Ceramic Soc. Inc., Westerville, Ohio, 1989) pp. 3–16.
3. D. D. MARCHANT and T. E. NEMECEK, ibid. pp. 19–54.
4. Y. KUROKAWA, K. UTSUMI, H. TAKAMIZWA, T. KAMATA and S. NOGUCHI, IEEE Trans. Comp. Hybrids Manuf. Technol. 8 (2) (1985) 247.
5. B. S.CHIOU, G. H. CHANG and J. G. DUH, Printing and surface Finishing 80 (1993) 65
6. J. H .CHANG, J. G. DUH and B. S. CHIOU, IEEE Trans. Comp. Hybrids Manuf. Technol. 16 (8) (1993) 1012.
7. B. S. CHIOU, K. C. LIU, J. G. DUH and P. S. PALANI-SAMY, T ibid. 13 (2) (1990) 267.
8. B. S. CHIOU, K. C. LIU, J. G. DUH and P. S. PALANI-SAMY, ibid. 14 (1991) 233.
9. G. D. O'CLOCK Jr, M. S. PETERS, J. R. PATTER, G. A. KLEESE, and R. V. MARTINI, ibid. 10 (1) (1987) 82.
10. P. W. DEHAVEN Mater. Res. Soc. Symp. Proc. 40 (1985) 123.
11. D. S. DUNN, T. F. MARINIS, W. M. SHERRY , and C. J. WILLIAMS, ibid. 40 (1985) 129..
12. C. W. ALLEN, M. R. FULCHER, A. S. RAI, G. A. SARGENT and A. E. MILLER, ibid. 40 (1985) 139.
13. R. J. GECKLE, IEEE Trans. on Comp. Hybrids Manuf. Technol. 14 (4) (1991) 691.
14. B. S. CHIOU, J. H. CHANG and J. G. DUH, IEEE Trans. Comp. Hybrids Manuf. Technol./Advanced packaging, submitted.
15. P. E. LILEY, R. C. REID and E. BUCK, "Perry's chemical engineers' handbook", 6th edition, edited by R. H. RERRY and D. GREEN (McGraw-Hill. U S A, 1984) p. 104.
16. H. H.MANKO, "Solders and soldering: Materials, production and analysis for reliable bonding", 2nd edition (McGraw-Hill, USA, 1979) p. 133.